THE JOURNAL OF BIOLOGICAL CHEMISTRY VOL. 285, NO. 26, pp. 19785–19792, June 25, 2010

Nitric Oxide Binds to the Proximal Heme Coordination Site of the Ferrocytochrome *c*/Cardiolipin Complex

FORMATION MECHANISM AND DYNAMICS[*][S]

Received for publication, September 18, 2009, and in revised form, April 1, 2010 Published, JBC Papers in Press, April 15, 2010, DOI 10.1074/jbc.M109.067736

Gary Silkstone[‡], Sofia M. Kapetanaki[§¶], Ivan Husu[‡], Marten H. Vos[§¶], and Michael T. Wilson[‡1]

From the [‡]Department of Biological Sciences, Wivenhoe Park, University of Essex, Colchester CO4 3SQ, United Kingdom, the [§]Laboratory for Optical Biosciences, CNRS Ecole Polytechnique, 91128 Palaiseau, France, and [¶]INSERM U696, 91128 Palaiseau, France

Mammalian mitochondrial cytochrome *c* interacts with cardiolipin to form a complex (cyt. *c*/CL) important in apoptosis. Here we show that this interaction leads to structural changes in ferrocytochrome *c* that leads to an open coordinate site on the central iron, resulting from the dissociation of the intrinsic methionine residue, where NO can rapidly bind ($k = 1.2 \times 10^7$ M^{-1} s^{-1}). Accompanying NO binding, the proximal histidine dissociates leaving the heme pentacoordinate, in contrast to the hexacoordinate nitrosyl adducts of native ferrocytochrome *c* or of the protein in which the coordinating methionine is removed by chemical modification or mutation. We present the results of stopped-flow and photolysis experiments that show that following initial NO binding to the heme, there ensues an unusually complex set of kinetic steps. The spectral changes associated with these kinetic transitions, together with their dependence on NO concentration, have been determined and lead us to conclude that NO binding to cyt. *c*/CL takes place via an overall scheme comparable to that described for cytochrome *c*′ and guanylate cyclase, the final product being one in which NO resides on the proximal side of the heme. In addition, novel features not observed before in other heme proteins forming pentacoordinate nitrosyl species, include a high yield of NO escape after dissociation, rapid (<1 ms) dissociation of proximal histidine upon NO binding and its very fast binding (60 ps) after NO dissociation, and the formation of a hexacoordinate intermediate. These features all point at a remarkable mobility of the proximal heme environment induced by cardiolipin.

Nitric oxide (NO) is an important signaling molecule that plays a key role in a variety of biological processes including vasodilation, neuronal function, inflammation, and immune function (1). Recently, it has been demonstrated that it is also involved in the regulation of apoptosis (programmed cell death), having a dual role, stimulatory in some cells and inhibitory in others, through mechanisms not fully elucidated (2, 3). Because of its hydrophobic nature, which enables easy diffusion in biomembranes (4, 5), NO can reach mitochondria, where it may also be produced by the recently discovered mitochondrial nitric-oxide synthase (6, 7). It has been shown that during apoptosis NO nitrosylates the heme iron of mitochondrial cytochrome *c* (cyt. *c*),[2] which is then rapidly released into the cytoplasm (8, 9), suggesting that NO may play a significant role in one of the key apoptotic events, the release of cyt. *c* (10). NO is a versatile ligand able to bind to both heme iron(II) and iron(III) states. It can give rise to 6-coordinate heme adducts as in myoglobin and hemoglobin with histidine and NO as distal axial ligands or to 5-coordinate heme adducts with NO as the axial ligand, as in sGC (guanylate cyclase) (11) and AXCP (cyt. *c*′ from *Alcaligenes xylosoxidans*) (12, 13). In AXCP, it can bind to the proximal side of the heme replacing the endogenous proximal His (13, 14), suggesting that heme-based sensor proteins may utilize both sides of their hemes for ligand discrimination.

Cyt. *c* is a small redox heme protein located in the mitochondrial intermembrane space (IMS), where it shuttles electrons between the complexes III (bc_1 complex) and IV (cytochrome *c* oxidase) of the respiratory chain. It bears a positive charge at pH values found in the IMS and thus interacts electrostatically with phospholipids bearing a net negative charge, such as cardiolipin (CL), a mitochondria-specific phospholipid (15). Moreover, it has been suggested that cyt. *c* (in a fraction of the molecules) may also be anchored to the outer surface of the mitochondrial inner membrane by hydrophobic interactions with CL. Upon interaction with CL, cyt. *c* has been shown to alter its tertiary structure and to display a peroxidase activity that results in the oxidation of CL and subsequently in the permeabilization of the outer mitochondrial membrane (16). This gain of peroxidatic function by cyt. *c* upon interaction with CL has been the focus of intense research effort that has recently been reviewed by Kagan *et al.* (17).

Our recent work has demonstrated that cyt. *c* in the presence of CL gains the capacity to bind CO rapidly and with high affinity, in sharp contrast to the CL-free protein (18). Furthermore, the CO dynamics of the cyt. *c*/CL complex indicate that significant conformational changes take place in the presence of CL, leading to the formation of channels that may facilitate the access of H_2O_2 to the heme, enabling the peroxidase activity of the cyt. *c*/CL complex (18) and pointing toward a possible regulatory role for carbon monoxide. Such a regulatory role has also been proposed for nitric oxide, which has been shown to

* This work was supported in part by grants from the Région Ile-de-France (to S. M. K.), from the Italian Government (to I. H.), and from BBSRC, UK (to M. T. W. and G. S.).

[S] The on-line version of this article (available at http://www.jbc.org) contains supplemental Fig. S1.

[1] To whom correspondence should be addressed: Dept. of Biological Sciences, Wivenhoe Park, University of Essex, Colchester CO4 3SQ, UK. Tel.: 441206872538; Fax: 441206872592; E-mail: wilsmt@essex.ac.uk.

[2] The abbreviations used are: cyt. *c*, cytochrome *c*; MOPS, 4-morpholinepropanesulfonic acid; CL, cardiolipin; cm, carboxymethyl; AXCP, cyt. *c*′ from *A. xylosoxidans*.

inhibit the peroxidase activity of the cyt. *c*/CL complex, with CL facilitating the interaction of cyt. *c* with NO (19).

Study of the NO binding dynamics can provide significant information about the heme environment, because these are closely related to the protein function and subtly controlled by the protein structure (20). In the present work, we investigated the NO release and binding dynamics, on time scales ranging from picoseconds to seconds, of the cyt. *c*/CL complex to gain further insight into the possible roles of NO in modulating cyt. *c*/CL-mediated apoptosis. We show that NO fully replaces the proximal histidine via an unusually complex set of kinetic steps, pointing at a remarkable mobility of the heme environment induced by CL. Our work implies that CL may contribute to a controlled NO release in mitochondria during the early stages of apoptosis.

EXPERIMENTAL PROCEDURES

Sample Preparation—Cyt. *c* (horse heart) was purchased from Aldrich and dissolved in either 20 mM MOPS, pH 6.7 (femtosecond spectroscopy, similar results were obtained with 20 mM Hepes pH 7.4) or 20 mM Hepes pH 7.4 (all other spectroscopy), and final protein concentrations were typically between 1 and 13 mM. Ferrous cyt. *c*/CL complexes (30 CL/cyt. *c*) were prepared as described (18). For the femtosecond measurements, the cyt. *c*/CL complex was equilibrated with ~0.1 atm of pure NO gas. For all other experiments stock NO solutions were prepared using an NO donor called Proli-NONOate purchased from Alexis Biochemicals. The concentration of stock NO solutions was determined using an extinction coefficient of 8,500 M^{-1} cm^{-1} at 250 nm. To study the reversibility of the process, returning the CL pentacoordinate nitrosyl adduct to the native cyt. *c* protein, CL was removed from the NO cyt. *c*/CL adduct by incubation (5 min) with 250 mM NaCl (Sigma) and 10 mM Triton X-100 (Sigma), and the NO was removed by photolysis in the presence of the NO scavenger carboxy-PTIO (Alexis Biochemicals). The protein was separated from the mixture by elution from a cation ion exchange resin (CM-52, Sigma). The sample of the resulting protein was then diluted to a concentration comparable to that of a sample of native ferrous cyt. *c* for spectral comparison (see "Results"). Ferrous carboxymethyl (cm) cyt. *c* was prepared as described (21).

Spectroscopy—Steady-state spectra were recorded using either a Shimadzu UV-Vis 1601 or Varian CARY 5E spectrophotometer. Multicolor femtosecond absorption spectroscopy using 60-fs pulses centered at 560 nm and white light continuum probe pulses in the 380–480 nm region, at a repetition rate of 30 Hz, and data analysis was performed as described (22). Stopped-flow spectroscopy was carried out using an Applied Photophysics SX-20 instrument. To obtain high quality data over a spectral range (here 380–450 nm) we did not employ a diode array for the experiments reported here, but instead accumulated kinetic traces using photomultiplier detection at 2-nm intervals throughout the wavelength range explored and used the whole data set to construct the time resolved spectra. Thus each experiment required 36 individual "shots" which on assembly yielded kinetic data points at 25-μs intervals (for the fastest time courses) and at 2-nm intervals on the wavelength scale. Microsecond laser flash photolysis measurements were carried out on an Applied Photophysics SX.18MV instrument. All optical spectroscopic measurements were performed at room temperature. Wilmad SQ EPR tubes were used for EPR samples. Tubes containing protein solutions were quickly frozen in methanol kept on dry ice. Once frozen, samples were transferred to liquid nitrogen where they were stored prior to measurements. The spectra were measured on a Bruker EMX EPR spectrophotometer equipped with an Oxford Instruments liquid helium system. A spherical high quality Bruker resonator SP9703 was used. Temperature for all samples was 10 K. Microwave frequency and power for all samples was 9.47 GHz and 3.18 milliwatts, respectively.

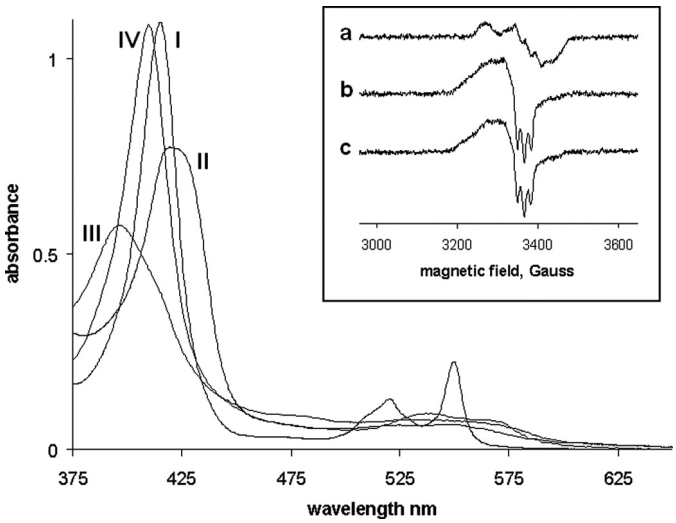

FIGURE 1. **Spectra of cyt. *c* (native) and cm cyt. *c*.** *I*, the dithionite reduced (deoxy) form of cyt. *c*; *II*, the deoxy form of cyt. *c*/CL; *III*, the deoxy form of cyt. *c*/CL/NO; *IV*, the deoxy form of cm cyt. *c*/NO. Conditions: [cyt. *c*] = 8 μM, [CL] = 240 μM, [NO] = 100 μM. *Inset*, EPR spectra of native and cm cyt. *c* (*a*) cm cyt. *c* + NO (the spectrum for M80A cyt *c* + NO was identical) (*b*) cm cyt. *c* + CL + NO (*c*) cyt. *c* + CL + NO. Conditions: [cyt. *c*] = 20 μM, [CL] = 500 μM, [NO] = 100 μM, temperature for all samples was 10 K and microwave frequency and power for all samples was 9.47 GHz and 3.18 milliwatt, respectively.

RESULTS

Static Spectra—The spectrum of the CL complex of ferro cyt. *c* is shown in Fig. 1. This spectrum has been assigned to a high spin pentacoordinate form of the heme (18). On binding NO to this complex, the broad Soret band of the ferrous form shifts to 394 nm and reduces in intensity, and this is accompanied by small changes in the visible region. These spectral changes are consistent with NO (12) binding to the heme to generate a pentacoordinate NO adduct. The spectrum is reminiscent to the absorption spectra of NO-bound guanylate cyclase (11), H93G myoglobin (23), and AXCP (12), indicating that the NO-bound form of the ferrous cyt. *c*/CL complex is 5-coordinated with neither the distal Met-80 nor proximal His-18 coordinated to the heme iron. This behavior may be contrasted with that of cm cyt. *c* (spectra not shown) or the yeast variant M80A mutant which binds NO, but yields a spectrum consistent with a hexacoordinate NO adduct (21).

These assignments are supported by the EPR spectra that are reported in the *inset* to Fig. 1. The NO adduct of cm cyt. *c* (and of the M80A mutant) show the typical "nine" line spectrum of the hexacoordinate species in which the unpaired electron on

the NO couples to the histidine nitrogen that coordinates to the iron trans to the NO. In contrast to this, and consistent with the optical spectrum, the NO adduct of the CL complex of ferro cyt. *c* exhibits a "three" line spectrum and the nine line spectrum is absent, indicative of full histidine displacement from the heme. Under different experimental conditions, Vlasova *et al.* (19) previously reported formation of a mixture of 5-coordinate and 6-coordinate cyt. *c*/NO complexes in the presence of CL. Interestingly, the CL complex of cm cyt. *c* also shows a three line EPR spectrum highlighting that CL does more than just displace the Met-80 from its coordination to the heme.

We further investigated the reversibility of the process returning the CL pentacoordinate nitrosyl adduct to the native cyt. *c* protein. Following the removal of NO by photolysis in the presence of an NO scavenger, and the separation of CL from cyt. *c* by addition of salt/detergent and cation exchange chromatography, the spectrum of the resulting protein in its reduced form was identical to that of native ferro cyt. *c* (data shown in SI). This result provides clear evidence that the transition brought about by CL is fully reversible. This experiment is also fully consistent with our finding that addition of salt stops rebinding of CO after laser photolysis, *i.e.* removal of CL returns the ferrous protein to its non CO binding native form (18).

Stopped-flow Experiments—On mixing the ferro cyt. *c*/CL adduct with excess NO a complex sequence of kinetic events was observed, in which a number of distinct spectral intermediates could be discerned. Fig. 2 shows the spectral evolution observed on mixing 15 μM NO with anaerobic ferro cyt. *c*/CL (2.5 μM cyt. *c*). The initial spectrum is captured 1.5 ms after mixing and thereafter a series of optical transitions takes place leading eventually, after ~20 s, to the final spectrum that is identical to that observed in static experiments (Fig. 1). In Fig. 2, a subset of the total data set collected is displayed. The data set was analyzed using an SVD algorithm and spectra generated for a sequential pathway with five species (A to E, including the initial and final forms and three intermediates). These spectra are also given in Fig. 2 together with the static ($t = 0$) deoxy spectrum.

The full time courses, displayed using a split time base at a single wavelength, 420 nm, and at two NO concentrations are given in Fig. 3. These time courses display the distinct phases that are temporally well separated. These phases and the putative assignments are now described in turn and for ease of understanding we refer also to the mechanism shown in Fig. 4.

The first very rapid kinetic process (within the first 50 ms) is, at high NO concentrations, partially lost in the dead time of the apparatus (1 ms). However the shape of the difference spectrum (static minus first captured spectrum, A*) is identical to that of the difference spectrum (A* minus the spectrum recorded at 50 ms), data not shown. This indicates that no other spectral process was missed. The rate constant of this first step was NO concentration dependent. This step we therefore assign to the initial NO binding to the heme. Kinetic analysis yields a second order rate constant k_1 of $2 \times 10^7\ \mathrm{M}^{-1}\,\mathrm{s}^{-1}$, very much in line with rate constants of NO binding to many other heme proteins, but interestingly orders of magnitude higher than binding to AXCP (24) and ferro M80A cyt. *c* (22) in which binding is

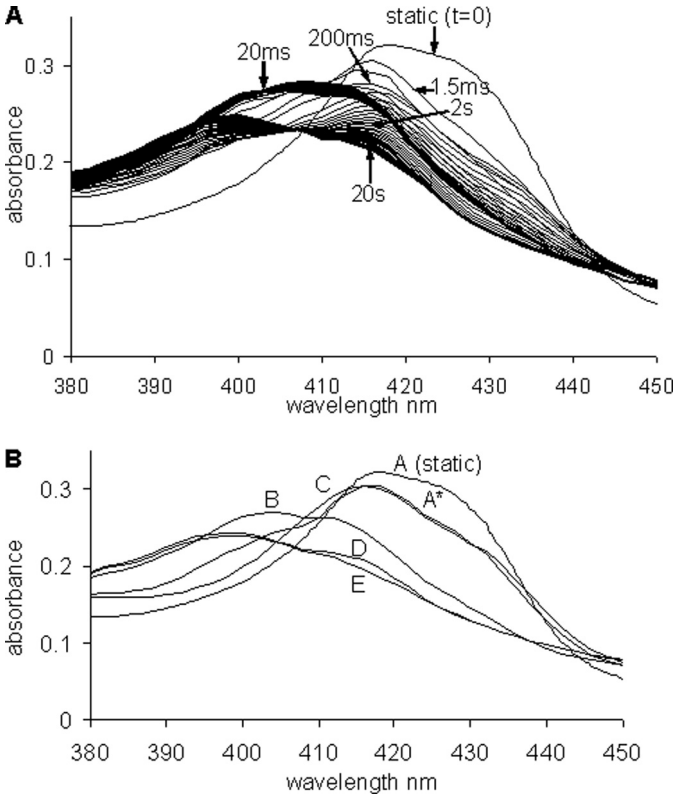

FIGURE 2. **Stopped-flow data for the mixing of the ferrous cyt. *c*/CL adduct with NO.** *A*, shown is the static ($t = 0$) deoxy spectra prior to mixing and the time-recorded spectra from ~1.5 ms after mixing to ~50 ms (spectra shown every ~1.8 ms) and from 50 ms to ~20 s (spectra shown every ~300 ms). Time indications are given at ~1.5 ms, 20 ms, 200 ms, 2 s, and 20 s. *B*, spectra A to E are from the global analysis of the stopped flow reaction between the ferrous cyt. *c*/CL adduct with NO (the static or $t = 0$ s spectra is also given). Conditions: [cyt. *c*] = 3 μM, [CL] = 75 μM, [NO] = 60 μM (all after mixing).

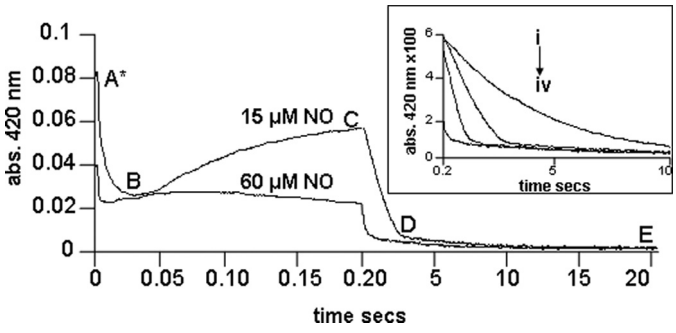

FIGURE 3. **Shown are the time courses for the stopped-flow reactions mixing the ferrous cyt. *c*/CL adduct with NO of different concentrations, followed at a single wavelength of 420 nm.** Time is shown on an isometric scale. [NO] used was ~60 and 15 μM after mixing. *Inset*, the time courses of four separate mixing reactions, cyt. *c*/CL with different NO concentrations. Time is plotted on an isometric time scale ranging from 0.2 to 10 s. Conditions: [cyt. *c*] = 3 μM, [CL] = 75 μM, [NO] = 7.5, 15, 30, and 60 μM all after mixing (i to iv, respectively), temperature, 22 °C, buffer used was 20 mM Hepes pH 7.4.

rate limited by steric hindrance provided by the tightly packed protein cage. The spectral changes accompanying NO binding indicate that the primary binding process leads to a species that is similar to the final NO bound form and different from the NO adducts of cm cyt. *c* or the M80X mutants that we have previously described (22) and shown to be hexacoordinate complexes (Fig. 1). Thus we propose that

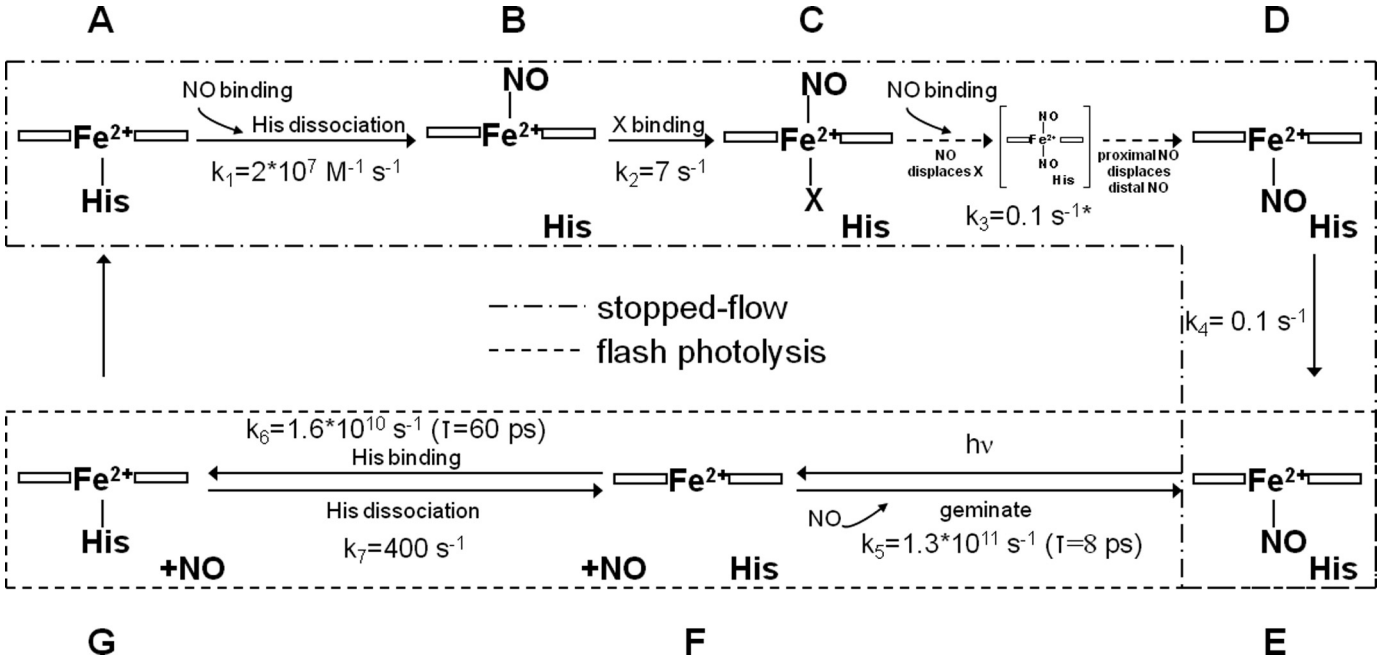

FIGURE 4. **Scheme of intermediates in the reactions between the ferrous cyt. *c*/CL complex and NO.** See text for details. *, this reaction is a zero-order reaction with a rate (Δ[cyt. *c*]/s.) proportional to the NO concentration. This observation may be expressed by incorporating the [NO] dependence into the rate constant. Thus, the rate constant may be written (Δ[cyt. *c*]/s)/[NO] which therefore has the units of s^{-1}, as given in the scheme.

the initial NO binding reaction dissociates the proximal histidine ligand to yield a pentacoordinate species. We see no evidence of a transient hexacoordinate species and thus conclude that dissociation of the histidine, once NO is bound to the heme, is more rapid (< 1 ms) than the binding.

Following the initial binding reaction a slower step occurs, the rate of which is essentially NO concentration independent. The amplitude of this phase is influenced by the NO concentration but we attribute this to the behavior of the subsequent step which more rapidly depletes this intermediate at high [NO], see later for details. Curiously, the second reaction takes the spectrum back toward that of the original spectrum, Fig. 2. This finding appears most easily explained by the binding of an, as yet unidentified, intrinsic ligand trans to the bound NO. If this conjecture is correct, the form of the spectrum suggests that the ligand is likely to be a weak field ligand as the spectrum is more reminiscent of a high spin rather than a low spin heme species.

The third major step is the most surprising for a variety of reasons. First this slow process is again NO concentration dependent, a remarkable feature given that second order processes in which NO binds to heme are generally very rapid. An important clue that may explain this phenomenon is that the time courses, especially at high NO concentrations, do not conform to exponentials. Rather, they are almost linear, typical of zero order steps (Fig. 3). Such time courses are seen in ligand binding to heme when the rate limit in the process is not chemical but diffusion (see "Discussion"). The spectrum of the species at the end of this process is very similar to the final product and by comparison we assign this to a pentacoordinate heme NO adduct. The last slow (k_4 = 0.1 s^{-1}), [NO] independent, step (D to E) takes the protein to the final NO adduct that we see in the static experiments.

The rate at which NO dissociates from the final complex was determined by mixing the NO adduct of the ferro cyt. *c*/CL complex with an excess of oxyhemoglobin, using the method described by Sarti *et al.* (25). The simultaneous formation of met hemoglobin and ferric cyt. *c* was followed by taking spectra in the visible region at known time intervals. A single exponential process was observed with rate constant ~5×10^{-4} s^{-1}.

Ultrafast Spectroscopy—On exposing the NO adduct of the ferro cyt. *c*/CL complex to a femtosecond laser pulse, NO dissociates from the heme. The spectral evolution at selected delay times of the ferrous-NO cyt. *c*/CL complex is presented in Fig. 5. The spectra are dominated by an induced absorption at 427 nm and the bleaching of the ground state at 394 nm. Global analysis of the data reveals a very fast component (~2.8 ps) ascribed to excited state photophysics (26, 27) and a 7-ps component ascribed to NO geminate recombination (*inset I*). The latter component has the same spectral characteristics as the 7.5-ps component of guanylate cyclase and corresponds to a 4-coordinated heme species (28). The static absorption spectrum of the 4-coordinated heme calculated as described under Ref. 29, is shown in *inset II*. Fitting of the kinetic trace at 427 nm (*inset III*) reveals that 11% of the NO does not rebind within 100 ps (*i.e.* the absorbance following photolysis falls from 10^{-2} A to 1.1×10^{-3} A, in 100 ps and only reaches zero in the ms time range). The remainder of the NO (89%) rebinds in a single exponential phase, indicating that NO remains close to the heme, without exploring multiple configurations in the heme pocket. The spectrum of the species remaining after the 7-ps component is significantly red-shifted with respect to the spectrum of the rebinding phase (Fig. 6*B*), and its extrema are similar to those of the steady-state difference spectrum and the microsecond difference spectrum (see below). Therefore, this spectrum is assigned to the 5-coordinate His-bound species. Thus, upon

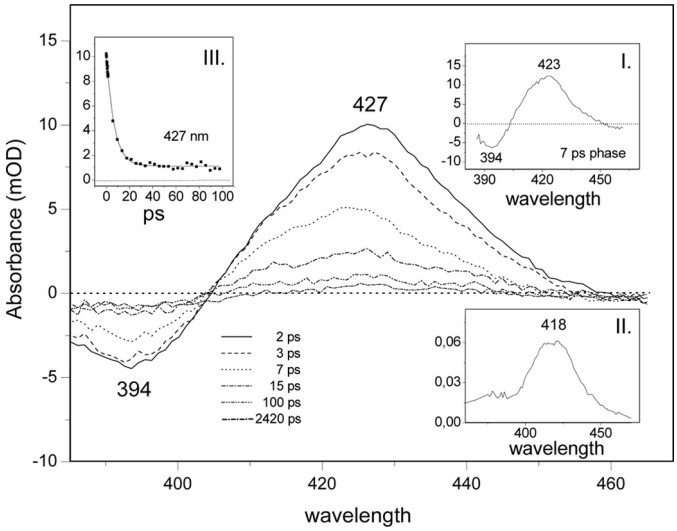

FIGURE 5. **Ultrafast spectroscopy of the ferrous-NO cyt. *c*/CL adduct.** The spectral evolution at selected delay times of the ferrous-NO cyt. *c*/CL adduct upon photodissociation of the NO is presented as a series of difference spectra using the spectrum of the NO form as a baseline. *Inset I*, spectral contribution of a 7-ps component (see "Results" for assignment). *Inset II*, the calculated static absorption spectrum of the 4-coordinated heme calculated (see "Results" for assignment). *Inset III*, a fit to the kinetic trace at 427 nm.

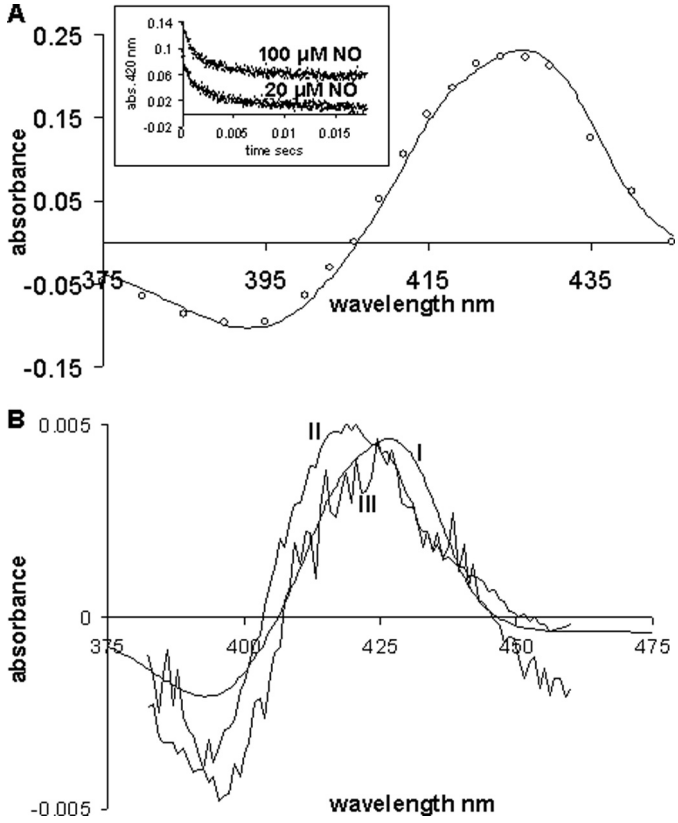

FIGURE 6. *A*, microsecond spectroscopy of the ferrous-NO cyt. *c*/CL adduct. The *line* represents the difference spectrum obtained from the steady-state species, the spectrum of the deoxy ferrous cyt. *c*/CL complex minus the spectrum of the NO adduct. The *circles* represent the difference spectrum constructed (375–450 nm, every 5 nm inclusive) on photodissociation of NO from its adduct with cyt. *c*/CL. At each wavelength, the total change in absorbance for each time course was plotted (is deoxy minus NO). This difference spectrum (by flash) is normalized (~×3) to the steady state one. *Inset*, time courses following flash photolysis of NO from its adduct with cyt. *c*/CL monitored at 420 nm and at two different NO concentrations 20 and 100 μM (offset for clarity) (similar results for 500 μM). *B*, *spectrum I*, the difference spectrum obtained from the steady state spectra of ferrous cyt. *c*/CL minus the spectra of the NO adduct (same as *A*, line). This spectrum has been multiplied by 0.2 to normalize it with spectra II and III. *Spectrum II*, the difference spectrum constructed of the 4-coordinate species corresponding to the 7-ps rebinding phase *inset I*. *Spectrum III*, the spectrum of the long-lived phase, assigned to 5-coordinate His-bound heme.

NO dissociation, binding of proximal His occurs in direct competition with NO rebinding, and the intrinsic time constant of the process (yield ~11%) is ~70 ps. No further spectral evolution takes place up to 4 ns, the longest time accessible with the instrument.

Microsecond Spectroscopy—The time courses observed following NO photodissociation from the ferro cyt. *c*/CL complex are shown in Fig. 6 (*inset*) at two NO concentrations. These time courses conform to simple exponentials yielding first order rate constants of ~400 s^{-1} that are [NO] concentration independent. The difference spectrum for the rebinding of NO, compiled by plotting the amplitude of these time courses as a function of wavelength, is given in Fig. 6*A* where it is compared with the corresponding static difference spectrum (*i.e.* deoxy spectrum minus NO adduct spectrum). It is clear from Fig. 6 that the kinetic and static difference spectra are identical, indicating that NO re-binding on this timescale is to a pentacoordinate heme that has histidine bound (see above). This accounts for the NO concentration-independent binding kinetics, which reflects replacement of the intrinsic ligand by NO, rate limited by the off-rate of the histidine.

DISCUSSION

The sequence of events that accompany NO binding to ferro cyt. *c*/CL is complex and in several ways unexpected. Mechanisms for NO binding to AXCP have been reported with similar mechanistic steps, albeit characterized by rather different kinetics and some different experimentally observable intermediates. These mechanisms, supported by x-ray structural information, are framed in terms of NO binding to a pentacoordinate *c* type heme, histidine displacement from the co-ordination site trans to the bound NO, binding of a second NO to the proximal site, from which the histidine has dissociated, to form a transient species in which two NO molecules are bound and finally the dissociation of the NO from the distal position, where the first NO bound, to form the final product, a pentacoordinate heme with NO bound at the proximal position (30, 31). We suggest that the spectral and kinetic data described above can best be understood in a related mechanistic framework, which is provided in Fig. 4. The scheme is delineated to show both, those species seen in the stopped flow experiments and those seen in photolysis experiments.

Species A we have characterized as a pentacoordinate ferrous form. The initial binding reaction with NO we represent as being to the empty distal side of the heme. This is the simplest hypothesis as the process is second order in NO and no other intermediates are seen. This is the site where CO binds. The spectrum of species B indicates that the intrinsic proximal histidine is dissociated on NO binding; we estimate a lower limit of the intrinsic rate constant of this process of ~10^3 s^{-1}. This process occurs orders of magnitude faster than in GC (32) and AXCP (33), where the proximal histidine is only dissociated

upon binding of a second NO molecule, and a transient pentacoordinate species is not observed. This comparison points at a high structural flexibility at the proximal heme site in the cyt. *c*/CL complex, allowing the dissociated histidine to easily move away from the heme iron interaction zone.

Subsequent to formation of the pentacoordinate species B a slower step leads to the formation of species C. Kinetics analysis (see "Results") of this process as part of a sequential mechanism (A>E) indicates that the rate constant for the formation of C is essentially [NO] independent with a rate constant k_2 of ~7 s^{-1}. This step is therefore not assigned to binding of a second NO molecule. Furthermore this step, most easily discerned at low [NO], is accompanied by a distinct and large change in spectrum, most readily explained by binding of a ligand to the heme to form a high spin species. There are a number of possibilities that may account for this spectrum. The most likely we suggest is binding of a weak field ligand to the empty proximal position of the heme. At present we are unable to identify this ligand or even to distinguish if it is an intrinsic amino acid residue or, for example, water. Such 6-coordinate nitrosyl intermediate has not been observed in GC or AXCP, where the proximal histidine remains bound longer (see above). At physiological, low, NO concentrations, this intermediate can be very long lived and possibly play a direct role in NO release in mitochondria.

Whatever the nature of this proximal ligand it appears to be displaced by a second NO molecule. The evidence for this conclusion comes from the strong dependence of the rate of formation of species D on [NO]. Two remarkable, but possible linked, features characterize this reaction. Firstly it is slow (timescale of a second), whereas binding of NO to ferrous heme is generally very rapid, secondly the time courses are, particularly at high [NO], not exponential but quasi-zero order typical for diffusive processes. To account for this behavior we propose that on initial mixing of the protein/lipid complex with NO this ligand rapidly binds to the empty distal site. Although the proximal histidine dissociates, the site vacated is inaccessible to NO until the protein has undergone some rearrangement as indicated by the steps described above, *i.e.* a reorganization allowing the binding of a ligand labeled X in Fig. 4 species C. NO in solution partitions into the considerable lipid phase that CL provides (30 CL molecules/cyt. *c*). It is from this phase, comprising bi-lipid membrane fragments on to which the cyt. *c* is bound, that NO now diffuses to the site where it can displace the putative ligand designated X. The rate of this process will depend on the concentration gradient and thus on [NO] but the process will not conform to a chemical kinetic process with exponential time course. Similar behavior has been described for CO combination with Hb in erythrocytes, rate limited by diffusion through the unstirred layer (34, 35). Clearly the access pathway of NO to the distal and to the proximal binding sites is very different in nature.

Given that the rate depends on the [NO] gradient, it follows that at high [NO], the time course will maintain its linearity over the majority of the binding process because the [NO] gradient changes little, and at lower [NO] this linearity is lost as the gradient now decreases during the time course. Thus, the initial slopes of the curves are directly proportional to the [NO] but at, say, ~7.5 μM [NO], the gradient falls as the NO is bound to the iron, which at ~3 μM removes the equivalent NO from solution leaving only ~4.5 μM free and thus a gradient of only ~1.5 μM.

If we ignore the non-exponential nature of the transition from C to D and assume that what we follow is not diffusion dependent but a reflection of the chemistry then there are a number of alternatives in assigning the relative values of rate constants. One alternative is that the formation of the dinitrosyl complex limits the overall processes and thus rate of the appearance of species D is [NO] dependent with second order rate constant of the order 10^4 M^{-1} s^{-1}, which is exceedingly small for NO binding to a ferrous heme, making this explanation unlikely in our view although not impossible.

The dominant feature of the transition from C to D is, therefore, the slow zero order phase. However, the situation may be more complex than described above. Simulations of the mechanism incorporating a zero order phase (not shown here), while reproducing the main features we observe do not fully model the change in amplitude in the signal assigned to the formation and decay of intermediate C seen on changing the [NO] from 30 to 60 μM. It is possible that there is a further component of the time course which is [NO] dependent and exponential and which is not therefore diffusion limited. For example, NO may access the heme site, in a fraction of the molecules at least, from the bulk solution and therefore display exponential kinetics. At high [NO] this process may effectively compete with the binding of the internal ligand (X in Fig. 4) and lead to the formation of D without passing through C. It may also, at lower [NO], smooth the transition between the zero order phase and the slow transition leading to D.

In agreement with Andrew *et al.* (33), who report NO binding to AXCP, we suggest a putative di-nitrosyl complex is transiently formed from which NO at the distal site dissociates to leave a nitrosyl complex with a single NO molecule bound at the proximal site. This is identical to the final product of NO binding to AXCP. Thus species D displays the spectrum typical for a pentacoordinate NO species and accounts for the similarity between the spectra of species D and B.

A final slow first order step associated with a small spectral change leads to the final stable product seen statically, this product is labeled E in Fig. 4 and is, as stated above, a pentacoordinated nitrosyl displaying optical and EPR spectra typical of such species. The nature of this final transition is presently unknown, but the small spectral changes are not compatible with ligand change at the iron, and thus we suggest that it reflects some slow structural relaxation of the lipid/protein complex bringing the heme environment to its final equilibrium state.

Species E is the starting point for all photolysis experiments. Dissociation of NO from this yields a 4-coordinate species, F, the spectrum for this species (Fig. 5, *Inset II*) has been constructed from the absolute absorption of species E, *i.e.* the static spectrum of the NO complex (Fig. 1) and the difference spectrum between species F and E given in Fig. 5. Rebinding to F is largely geminate (89%) with a time constant typical for geminate recombination of NO to heme *c* of 8 ps (20). The remainder of the NO moves away from the heme, our data to date do not allow us to say whether this NO reaches the bulk phase or moves to sites removed from the heme but within the protein/

lipid complex, but the latter seems the more likely (see below). Nevertheless, the fact that 11% of the NO does not rebind in the geminate phase may indicate a higher apparent quantum yield, φ, (fraction of NO dissociated leaving the heme pocket) for NO dissociation than is usual for heme proteins. In particular, it is much higher than in GC (~3%) (28) and AXCP (~1%) (31). The high probability of escape may be due to the very efficient and direct competition of His binding (τ = ~60 ps). Indeed, recent experiments on AXCP indicate that in this protein no such direct competition exists and NO has to leave the heme environment before His can bind (36). Again, this comparison points at a flexible proximal binding environment of the heme in the cyt. *c*/CL complex, allowing for accommodation of both NO and His in the proximity of the heme iron. We also note that the relatively high φ for NO dissociation mirrors the high quantum yield for CO dissociation (φ = 0.89) that we have reported for the cyt. *c*/CL complex (18).

The binding of His yields species G, the pentacoordinate complex, to which NO recombines at the rate of the histidine dissociation ($k_7 = 400\ s^{-1}$). The fact that NO re-binding following photodissociation is rate limited at 400 s^{-1} while CO rebinding in similar experiments is not limited at this value and proceeds at high [CO] more rapidly (18), strongly supports the view that binding of NO is coupled to structural changes not encountered with CO and is consistent with these gaseous ligands rebinding to opposite faces of the heme group.

The final step (G to A) is added to counterbalance the slow "rearrangement" we have assigned to the transition within the nitrosyl complex from D to E, presuming that some similar step may occur in the deoxy ferrous state that we have been unable to see because we only form G following NO dissociation and this species is removed on recombination with NO following histidine replacement. The distinction between G and A also appears necessary if we are to explain the differences between NO binding seen in mixing or photolysis experiments (see below).

Given the complexities of the reaction we observe, and given the precedent of AXCP, we believe that the mechanism depicted in Fig. 4 is the simplest that is consistent with all the data. There are several questions that may legitimately be posed regarding this mechanism. Why, for example, given the seemingly similar structure of species A and G do they display such different NO binding profiles. We suggest an answer to this in terms of the NO moving, following dissociation from the proximal side, into the protein but being retained near the binding site. In this view, the 400 s^{-1} NO rebinding formally corresponds to a geminate heme-NO rebinding process. We must also suppose that binding to the distal side in G is denied to the NO, at least in the time frame we monitor, by those structural changes that we assign to the D to E transition. It is also for this reason that we propose a transition between G and A in the scheme reversing the transition D to E and completing the thermodynamic cycle.

The findings we report here demonstrate the remarkable influence CL exerts on the ligand binding properties of cyt. *c* and in particular on ferro cyt. *c* which in the absence of CL does not bind CO and binds NO only very slowly. CL has been suggested to bind to cyt. *c* both through electrostatic interactions and through hydrophobic interactions between one of the aliphatic chains and a non polar cleft formed in the surface of the protein by the parallel strands of the polypeptide backbone (37). This interaction triggers significant structural alteration in the protein. Most obviously the Met-80 residue is removed from coordination to the iron allowing facile NO (and CO) binding but over and above this, conformational changes are promoted that lead to the dissociation of the proximal histidine residue on NO binding (Fig. 1). This conversion of a hexacoordinate to a pentacoordinate heme nitrosyl complex on interaction with an "effector" finds parallels in the interaction of hemoglobin NO complexes with IHP (inositol hexaphosphate, a mimic of the *in vivo* effector 2,3 bis-phosphoglycerate), where the proximal histidine in the α-chains dissociates (38). It is unknown whether here NO binds to the proximal or distal side. The major conclusion that NO binds finally to the proximal position is surprising and may have important functional significance not only through modulating NO release in the mitochondria but also by interfering with the peroxidatic activity of protein.

Our data also reveal that following photo-dissociation a significant fraction of the dissociated NO ligand escapes from the heme cavity of the cyt. *c*/CL complex. This is consistent with our previous studies on the CO dynamics of the cyt. *c*/CL complex that indicated that significant conformational changes occurred in cyt. *c* on interaction with CL resulting in heme pocket reorganization coupled with dissociation of the intrinsic methionine heme ligand (18). This in itself may have important consequences as recent work has shown that disruption of the methionine to Fe ligation stimulates translocation of cyt. *c* to the cytoplasm and nucleus in non-apoptotic cells (39). In addition, we propose that NO binds to the heme through a complex mechanism that is in principle similar to that proposed for AXCP (31), but with a number of remarkable kinetic and intermediate differences, pointing in particular to a very flexible, yet confined, proximal heme pocket. The functional consequences of this complex behavior, were it to occur *in vivo*, are presently unclear, however, we may, by comparison with AXCP and guanylate cyclase, suggest that this behavior may reflect a kinetic trap mechanism for the release of NO from ferrous cyt. *c*/CL complex. In our experiments we have also identified a relatively long-lived pentacoordinate species with NO bound to the distal side. We do not know as yet the dissociation rate from this form but this form as well as the hexacoordinate NO-bound intermediate may also play a role in regulating NO release in mitochondria. Our work therefore implies that CL may contribute to a controlled NO release in mitochondria during the early stages of apoptosis.

Acknowledgments—We thank Dr. Ursula Liebl for critical reading of the manuscript and Dr. Dimitri Svistunenko for help with EPR experiments.

REFERENCES

1. Ignarro, L. J. (1990) *Pharmacol. Toxicol.* **67,** 1–7
2. Chung, H. T., Pae, H. O., Choi, B. M., Billiar, T. R., and Kim, Y. M. (2001) *Biochem. Biophys. Res. Commun.* **282,** 1075–1079
3. Choi, B. M., Pae, H. O., Jang, S. I., Kim, Y. M., and Chung, H. T. (2002) *J. Biochem. Mol. Biol.* **35,** 116–126
4. Radi, R., Cassina, A., Hodara, R., Quijano, C., and Castro, L. (2002) *Free*

Radical Biol. Med. **33,** 1451–1464
5. Rubbo, H., Radi, R., Trujillo, M., Telleri, R., Kalyanaraman, B., Barnes, S., Kirk, M., and Freeman, B. A. (1994) *J. Biol. Chem.* **269,** 26066–26075
6. Ghafourifar, P., and Cadenas, E. (2005) *Trends Pharmacol. Sci.* **26,** 190–195
7. Haynes, V., Elfering, S., Traaseth, N., and Giulivi, C. (2004) *J. Bioenerget. Biomembr.* **36,** 341–346
8. Schonhoff, C. M., Gaston, B., and Mannick, J. B. (2003) *J. Biol. Chem.* **278,** 18265–18270
9. Mannick, J. B., and Schonhoff, C. M. (2004) *Free Radic. Res.* **38,** 1–7
10. Orrenius, S., Gogvadze, V., and Zhivotovsky, B. (2007) *Annu. Rev. Pharmacol. Toxicol.* **47,** 143–183
11. Stone, J. R., and Marletta, M. A. (1994) *Biochemistry* **33,** 5636–5640
12. Yoshimura, T., Suzuki, S., Nakahara, A., Iwasaki, H., Masuko, M., and Matsubara, T. (1986) *Biochemistry* **25,** 2436–2442
13. Lawson, D. M., Stevenson, C. E., Andrew, C. R., and Eady, R. R. (2000) *EMBO J.* **19,** 5661–5671
14. Andrew, C. R., Green, E. L., Lawson, D. M., and Eady, R. R. (2001) *Biochemistry* **40,** 4115–4122
15. Iverson, S. L., and Orrenius, S. (2004) *Arch. Biochem. Biophys.* **423,** 37–46
16. Basova, L. V., Kurnikov, I. V., Wang, L., Ritov, V. B., Belikova, N. A., Vlasova, I. I., Pacheco, A. A., Winnica, D. E., Peterson, J., Bayir, H., Waldeck, D. H., and Kagan, V. E. (2007) *Biochemistry* **46,** 3423–3434
17. Kagan, V. E., Bayir, H. A., Belikova, N. A., Kapralov, A., Yyurina, Y. Y., Yyurin, V. A., Jiang, J., Stoyanovsky, D. A., Wipf, P., Kochanek, P. M., Greenberger, J. S., Pitt, B., Shvedova, A. A., and Borisenko, G. (2009) *Free Radical. Biol. Med.* **46,** 1439–1453
18. Kapetanaki, S. M., Silkstone, G., Husu, I., Liebl, U., Wilson, M. T., and Vos, M. H. (2009) *Biochemistry* **48,** 1613–1619
19. Vlasova, I. I., Tyurin, V. A., Kapralov, A. A., Kurnikov, I. V., Osipov, A. N., Potapovich, M. V., Stoyanovsky, D. A., and Kagan, V. E. (2006) *J. Biol. Chem.* **281,** 14554–14562
20. Vos, M. H. (2008) *Biochim. Biophys. Acta* **1777,** 15–31
21. Silkstone, G., Jasaitis, A., Vos, M. H., and Wilson, M. T. (2005) *Dalton Trans.* **21,** 3489–3494
22. Silkstone, G., Jasaitis, A., Wilson, M. T., and Vos, M. H. (2007) *J. Biol. Chem.* **282,** 1638–1649
23. Negrerie, M., Kruglik, S. G., Lambry, J. C., Vos, M. H., Martin, J. L., and Franzen, S. (2006) *J. Biol. Chem.* **281,** 10389–10398
24. Pixton, D. A., Petersen, C. A., Franke, A., van Eldik, R., Garton, E. M., and Andrew, C. R. (2009) *J. Am. Chem. Soc.* **131,** 4846–4853
25. Giuffrè, A., Forte, E., Brunori, M., and Sarti, P. (2005) *FEBS Lett.* **579,** 2528–2532
26. Petrich, J. W., Poyart, C., and Martin, J. L. (1988) *Biochemistry* **27,** 4049–4060
27. Franzen, S., Kiger, L., Poyart, C., and Martin, J. L. (2001) *Biophys. J.* **80,** 2372–2385
28. Négrerie, M., Bouzhir, L., Martin, J. L., and Liebl, U. (2001) *J. Biol. Chem.* **276,** 46815–46821
29. Ye, X., Demidov, A., and Champion, P. M. (2002) *J. Am. Chem. Soc.* **124,** 5914–5924
30. Andrew, C. R., Rodgers, K. R., and Eady, R. R. (2003) *J. Am. Chem. Soc.* **125,** 9548–9549
31. Kruglik, S. G., Lambry, J. C., Cianetti, S., Martin, J. L., Eady, R. R., Andrew, C. R., and Negrerie, M. (2007) *J. Biol. Chem.* **282,** 5053–5062
32. Zhao, Y., Brandish, P. E., Ballou, D. P., and Marletta, M. A. (1999) *Proc. Natl. Acad. Sci. U.S.A.* **96,** 14753–14758
33. Andrew, C. R., George, S. J., Lawson, D. M., and Eady, R. R. (2002) *Biochemistry* **41,** 2353–2360
34. Antonini, E., Brunori, M., Giardina, B., Benedetti, P. A., Bianchini, G., and Grassi, S. (1978) *FEBS Lett.* **86,** 209–212
35. Coletta, M., Alayash, A. I., Wilson, M. T., Benedetti, P. A., Evangelista, V., and Brunori, M. (1988) *FEBS Lett.* **236,** 127–131
36. Yoo, B. K., Martin, J. L., Andrew, C. R., and Negrerie, M. (2010) in *Rebinding of Proximal Histidine in the Cytochrome c′ from Alcaligenes xylosoxidans Acts as a Molecular Trap for Nitric Oxide* (Corkum, P., De Silvestri, S., Nelson, K. A., Riedle, E., and Schoenlein, R. W., eds), Ultrafast Phenomena XVI, Springer, Berlin
37. Kalanxhi, E., and Wallace, C. J. A. (2007) *Biochem. J.* **407,** 179–187
38. Perutz, M. F., Kilmartin, J. V., Nagai, K., Szabo, A., and Simon, S. R. (1976) *Biochemistry* **15,** 378–387
39. Godoy, L. C., Muñoz-Pinedo, C., Castro, L., Cardaci, S., Schonhoff, C. M., King, M., Tórtora, V., Marín, M., Miao, Q., Jiang, J. F., Kapralov, A., Jemmerson, R., Silkstone, G. G., Patel, J. N., Evans, J. E., Wilson, M. T., Green, D. R., Kagan, V. E., Radi, R., and Mannick, J. B. (2009) *Proc. Natl. Acad. Sci. U.S.A.* **106,** 2653–2658